N95-27361

A NAVIER-STOKES BOUNDARY ELEMENT SOLVER

404934

56-34

45109

p. 14

O. Lafe
Innovative Computing Group
OLTech Corporation
Chesterland, Ohio

D.R. Reddy
Internal Fluid Mechanics Division
NASA Lewis Research Center
Cleveland, Ohio

and

A. H-D. Cheng
Department of Civil Engineering
University of Delaware
Newark, Delaware

SUMMARY

Using global interpolation functions (GIFs), boundary element solutions are obtained for two-dimensional laminar flows. Two schemes are proposed for handling the convective terms. The first treats convection as a forcing function, and converts the flow equations to pseudo-Poisson equations. In the second scheme, some convective effect is incorporated into the fundamental solution used in constructing the pertinent integral equations. The lid-driven cavity flow is selected as the benchmark problem.

INTRODUCTION

The boundary element method (BEM) has traditionally been applied to problems governed by linear differential equations. At the core of the basic BEM computational process is the fundamental solution (also referred to as the free-space Green's function) defined as the impulse response of the governing equation to a unit action. This fundamental solution is either too difficult or impossible to derive for practical nonlinear problems. Recently, with the introduction of the so-called *Dual Reciprocity* techniques (see *e.g., Nardini & Brebbia* [1982]; *Brebbia et al.* [1991]; *Partridge et al.* [1992]; *Cheng et al.* [1993]; *Lafe* [1993]; *Lafe & Cheng* [1994]), the method is being proposed for certain classes of nonlinear problems.

Using the *Dual Reciprocity* approach, a given problem is typically decomposed into two parts - the linear and nonlinear portions. The solution to the linear portion is represented by a boundary integral whose kernel consists of the fundamental solution to the linear governing equation. The nonlinear part is represented by either 1) local bases functions (*Brebbia et al.*, [1991]); or 2) global interpolation functions (GIFS) (*Lafe* [1993]). In either case, the boundary integral expressions and interpolation functions contain coefficients whose values are to be determined by enforcing the boundary conditions. When the "direct BEM" approach is followed the unknown coefficients are in essence the unknown physical variables (velocity components, pressure, temperature) of the problem. On the other hand, using the "indirect BEM" approach, the unknown are the weights/strengths of the boundary sources/dipoles and the local/global interpolating functions. The computational intensity of the indirect approach is much less than for the direct.

In this paper, we develop a GIF-based indirect BEM code for two- dimensional steady-state incompressible Navier-Stokes equation. Test results are shown for the lid-driven cavity problem.

GOVERNING EQUATIONS

The governing equations are:

$$\frac{\partial u}{\partial x} + \frac{\partial v}{\partial y} = 0 \tag{1}$$

$$u\frac{\partial u}{\partial x} + v\frac{\partial u}{\partial y} = -\frac{1}{\rho}\frac{\partial p}{\partial x} + \frac{\mu}{\rho}\left(\frac{\partial^2 u}{\partial x^2} + \frac{\partial^2 u}{\partial y^2}\right) \tag{2}$$

$$u\frac{\partial v}{\partial x} + v\frac{\partial v}{\partial y} = -\frac{1}{\rho}\frac{\partial p}{\partial y} + \frac{\mu}{\rho}\left(\frac{\partial^2 v}{\partial x^2} + \frac{\partial^2 v}{\partial y^2}\right) \tag{3}$$

where (u, v) are the velocity components in the x and y directions respectively, p is the pressure, ρ is the density, and μ is the viscosity. Let

$$X = x/L$$

$$
\begin{aligned}
Y &= y/L \\
U &= u/\overline{v} \\
V &= v/\overline{v} \\
P &= p/\left(\rho\overline{v}^2\right)
\end{aligned}
$$

With these the governing equations become:

$$
\frac{\partial U}{\partial X} + \frac{\partial V}{\partial Y} = 0 \tag{4}
$$

$$
U\frac{\partial U}{\partial X} + V\frac{\partial U}{\partial Y} = -\frac{\partial P}{\partial X} + \frac{1}{R_e}\left(\frac{\partial^2 U}{\partial X^2} + \frac{\partial^2 U}{\partial Y^2}\right) \tag{5}
$$

$$
U\frac{\partial V}{\partial X} + V\frac{\partial V}{\partial Y} = -\frac{\partial P}{\partial Y} + \frac{1}{R_e}\left(\frac{\partial^2 V}{\partial X^2} + \frac{\partial^2 V}{\partial Y^2}\right) \tag{6}
$$

where the Reynold's Number $R_e = \rho\overline{v}L/\mu$.

BOUNDARY INTEGRAL EQUATIONS

In order to convert the above into boundary integral equations two approaches have been followed. In the first approach, the entire system of equations is converted into an elliptic system, with the convective term wholly embedded in the right-hand-side forcing function. There is concern about the suitability of the elliptic system to adequately represent the convective forces at moderate to high Reynold's number regimes. The second approach rectifies this through a more direct perturbation-based analysis which is more suited to capturing convective effects as the Reynold's number increases.

Approach I

The above equations are converted into an elliptic system:

$$
\nabla^2 U = F_1 \tag{7}
$$

$$
\nabla^2 V = F_2 \tag{8}
$$

$$
\nabla^2 P = F_3 \tag{9}
$$

where

$$
F_1 = R_e\left(U\frac{\partial U}{\partial X} + V\frac{\partial U}{\partial Y} + \frac{\partial P}{\partial X}\right)
$$

$$
\begin{aligned}
F_2 &= R_e\left(U\frac{\partial V}{\partial X}+V\frac{\partial V}{\partial Y}+\frac{\partial P}{\partial Y}\right) \qquad (10)\\
F_3 &= 2\left(\frac{\partial U}{\partial X}\frac{\partial V}{\partial Y}-\frac{\partial U}{\partial Y}\frac{\partial V}{\partial X}\right)
\end{aligned}
$$

Boundary Integral Equations

The associated indirect boundary integral equations are:

$$
\begin{aligned}
U(X,Y) &= \int_\Gamma w_1(X',Y')g(X',Y';X,Y)\,d\Gamma+\sum_k \beta_{1k}\Psi_k(X,Y) \qquad (11)\\
V(X,Y) &= \int_\Gamma w_2(X',Y')g(X',Y';X,Y)\,d\Gamma+\sum_k \beta_{2k}\Psi_k(X,Y) \qquad (12)\\
P(X,Y) &= \int_\Gamma w_3(X',Y')g(X',Y';X,Y)\,d\Gamma+\sum_k \beta_{3k}\Psi_k(X,Y) \qquad (13)
\end{aligned}
$$

in which

$$
\begin{aligned}
&g=\ln\left[(X-X')^2+(Y-Y')^2\right]\\
&\sum_k \beta_{ik}M_k(X,Y)=F_i(X,Y) \qquad (14)\\
&\nabla^2\Psi_k(X,Y)=M_k(X,Y)
\end{aligned}
$$

The functions $M_k(X,Y)$ are the interpolation functions used in representing the convective terms. If we choose

$$M_k = cos(m_kX)cos(n_kY) \qquad (15)$$

it is easily shown (*Lafe* [1993]) that

$$\Psi_k=\frac{cos(m_kX)cos(n_kY)}{(n_k^2+m_k^2)} \qquad (16)$$

Approach II

Our aim here is to have a better incorporation of the convective effects in the driving differential operator. Let

$$
\begin{aligned}
U &= U_0+U_1\\
V &= V_0+V_1\\
P &= P_0+P_1
\end{aligned}
$$

where (U_0, V_0, P_0) denote solutions to a convection-free flow field, while (U_1, V_1, P_1) represent the convective effects. Hence

$$\nabla^2 U_0 = 0 \tag{17}$$

$$\nabla^2 V_0 = 0 \tag{18}$$

$$\nabla^2 P_0 = 2\left[\frac{\partial U_0}{\partial X}\frac{\partial V_0}{\partial Y} - \frac{\partial U_0}{\partial Y}\frac{\partial V_0}{\partial X}\right] \tag{19}$$

while

$$\frac{1}{R_e}\nabla^2 U_1 - o_1(U_0, V_0, U_1, V_1, P_1) = f_1(U_0, V_0, P_0) + h_1(U_1, V_1) \tag{20}$$

$$\frac{1}{R_e}\nabla^2 V_1 - o_2(U_0, V_0, U_1, V_1, P_1) = f_2(U_0, V_0, P_0) + h_2(U_1, V_1) \tag{21}$$

$$\frac{1}{2}\nabla^2 P_1 - o_3(U_0, V_0, U_1, V_1, P_1) = h_3(U_1, V_1) \tag{22}$$

where

$$
\begin{aligned}
o_1 &= U_0\frac{\partial U_1}{\partial X} + \frac{\partial U_0}{\partial X}U_1 + V_0\frac{\partial U_1}{\partial Y} + \frac{\partial U_0}{\partial Y}V_1 + \frac{\partial P_1}{\partial X} \\
o_2 &= U_0\frac{\partial V_1}{\partial X} + \frac{\partial V_0}{\partial X}U_1 + V_0\frac{\partial V_1}{\partial Y} + \frac{\partial V_0}{\partial Y}V_1 + \frac{\partial P_1}{\partial Y} \\
o_3 &= \frac{\partial U_0}{\partial X}\frac{\partial V_1}{\partial Y} + \frac{\partial V_0}{\partial Y}\frac{\partial U_1}{\partial X} - \frac{\partial U_0}{\partial Y}\frac{\partial V_1}{\partial X} - \frac{\partial V_0}{\partial X}\frac{\partial U_1}{\partial Y} \\
f_1 &= U_0\frac{\partial U_0}{\partial X} + V_0\frac{\partial U_0}{\partial Y} + \frac{\partial P_0}{\partial X} \\
f_2 &= U_0\frac{\partial V_0}{\partial X} + V_0\frac{\partial V_0}{\partial Y} + \frac{\partial P_0}{\partial Y} \\
h_1 &= U_1\frac{\partial U_1}{\partial X} + V_1\frac{\partial U_1}{\partial Y} \\
h_2 &= U_1\frac{\partial V_1}{\partial X} + V_1\frac{\partial V_1}{\partial Y} \\
h_3 &= \frac{\partial U_1}{\partial X}\frac{\partial V_1}{\partial Y} - \frac{\partial U_1}{\partial Y}\frac{\partial V_1}{\partial X}
\end{aligned}
$$

The external boundary conditions are imposed on (U_0, V_0, P_0). Therefore the variables (U_1, V_1, P_1) are allowed to enjoy homogeneous boundary conditions.

Boundary Integral Equations

The velocity components (U_0, V_0), which are governed by Laplace's equations, can be represented by 'pure' boundary integral equation using the fundamental solution for potential flow. However the pressure term, because of the non-zero forcing function, will include global interpolation functions.

Therefore, the indirect boundary integral equations for the convection-free variables are:

$$U_0(X,Y) = \int_\Gamma w_{01}(X',Y')g(X',Y';X,Y)\, d\Gamma \tag{23}$$

$$V_0(X,Y) = \int_\Gamma w_{02}(X',Y')g(X',Y';X,Y)\, d\Gamma \tag{24}$$

$$P_0(X,Y) = \int_\Gamma w_{03}(X',Y')g(X',Y';X,Y)\, d\Gamma + \sum_k \beta_{0k}\Psi_k(X,Y) \tag{25}$$

where (w_{01}, w_{02}, w_{03}) are fictitious sources while Ψ_k are the GIFS.

The convective effects (U_1, V_1, P_1) are represented by GIFS. For flows in simple geometries it is possible to select GIFS which automatically satisfy the required homogeneous boundary conditions.

Hence

$$U_1(X,Y) = \sum_k \beta_{1k}\Psi_k(X,Y) \tag{26}$$

$$V_1(X,Y) = \sum_k \beta_{2k}\Psi_k(X,Y) \tag{27}$$

$$P_1(X,Y) = \sum_k \beta_{3k}\Psi_k(X,Y) \tag{28}$$

in which $(\beta_{1k}, \beta_{2k}, \beta_{3k})$ are the pertinent coefficients for the GIFS. These parameters are calculated by enforcing

1. Equations (20-22) at selected collocation points within the flow region and
2. Homogeneous conditions at selected boundary points.

The chief advantage of the first approach is the simplicity and size of the global coefficient matrices, derived from the Laplace equation solver. This translates into a compact, fast, and highly efficient numerical implementation. The drawback is its iterative character since the forcing function depends on the solution being sought. Convergence is difficult to achieve for large Reynold's number because the governing elliptic system becomes singular. and cannot adequately represent the underlying physics of the problem. The second approach. which in essence separates the convection-free flow from the main flow. allows for a more direct representation of the asymptotic limits of the Reynold's number. Furthermore. by products of higher-order terms (*i.e.*, setting $h1 = h2 = h3 = 0$. the solutions can be obtained without iteration. However. the coefficient matrix is larger and the approach involves a greater level of computational intensity.

NUMERICAL IMPLEMENTATION

Approach I

We subdivide the boundary into n_b elements. Let $N_k(\mathbf{x})$ $(k = 1, 2, \cdots n_b)$ represent the bases functions describing the distribution of w on Γ. In the examples being reported in this paper. constant bases functions are being used for the fictitious strengths w_i on the boundary. By selecting each of the n_b boundary points as successive origins of integration. the pertinent integral equations can be assembled into the system:

$$\sum_{k=1}^{n_b} a_{ik} w_k = b_i \qquad i = 1, 2, \cdots, n_b \tag{29}$$

where

$$a_{ik} = \begin{cases} \int_{\Gamma_k} N_k(\mathbf{x}') g(\mathbf{x}', \mathbf{x}_i)\, d\mathbf{x}' & \mathbf{x}_i \in \Gamma_\Phi \\ \int_{\Gamma_k} N_k(\mathbf{x}') \partial g / \partial n(\mathbf{x}', \mathbf{x}_i)\, d\mathbf{x}' & \mathbf{x}_i \in \Gamma_Q \end{cases} \tag{30}$$

$$b_i = \begin{cases} \Phi(\mathbf{x}_i) - \sum_{j=1}^{n_d} \beta_j \Psi_{ij} & \mathbf{x}_i \in \Gamma_\Phi \\ \partial\Phi/\partial n(\mathbf{x}_i) - \sum_{j=1}^{n_d} \beta_j \partial\Psi_{ij}/\partial n & \mathbf{x}_i \in \Gamma_Q \end{cases} \tag{31}$$

where $\Phi = (U, V, P)$. Therefore. we have n_b equations to determine w_k $(k = 1, 2, \cdots n_b)$. Symbolically equation (29) can be written in the alternative form:

$$\mathcal{A}\mathcal{W} = \mathcal{B} \tag{32}$$

which can be inverted to give:

$$\mathcal{W} = \mathcal{A}^{-1}\mathcal{B} \tag{33}$$

The whole process boils down to the iterative solution of equations (14) and (33), with repeated updating of **F** using (10). The iterative steps are:

1. Start with a trial **F** (*i.e.*, F_i values for $i = 1, 2, \cdots n_d$).
2. Obtain β from equation (14).
3. Obtain $\mathcal{W}$ using equation (33).
4. Use discretized forms of the appropriate integral equations to compute Φ, $\nabla\Phi$ at all n_d points. This provides a better estimate for **F**.
5. Go back to Step 2 if convergence condition is still unsatisfied.

Note that the matrix inversions in equations (14) and (33) need only be performed once, for fixed boundary problems. The vectors $\mathcal{W}$ and β are the quantities whose values change during the iterative process. Once convergence is reached, the discretized integral equations can be used routinely to obtain $\Phi = (U, V, P)$ or the gradient at any point ($\mathbf{x}$) of interest.

Approach II

The numerical implementation for the convection-free quantities (U_0, V_0, P_0) is similar to the one followed in Approach I, with the coefficients for the GIFS set to zero for the velocities. No iteration is required.

The convective-flow quantities are calculated through the coefficients $(\beta_{1k}, \beta_{2k}, \beta_{3k})$ whose values are obtained by solving the following coefficient matrices:

$$\sum_{k=1}^{n_T} \beta_{1k} A_{1ik} + \sum_{k=1}^{n_T} \beta_{1k} A_{2ik} + \sum_{k=1}^{n_T} \beta_{1k} A_{3ik} = F_{1i} \quad i = 1, 2, \cdots n_d \quad (34)$$

$$\sum_{k=1}^{n_T} \beta_{2k} B_{1ik} + \sum_{k=1}^{n_T} \beta_{2k} B_{2ik} + \sum_{k=1}^{n_T} \beta_{2k} B_{3ik} = F_{i2} \quad i = 1, 2, \cdots n_d \quad (35)$$

$$\sum_{k=1}^{n_T} \beta_{3k} C_{1ik} + \sum_{k=1}^{n_T} \beta_{3k} C_{2ik} + \sum_{k=1}^{n_T} \beta_{3k} C_{3ik} = F_{i3} \quad i = 1, 2, \cdots n_d \quad (36)$$

$$\sum_{k=1}^{n_T} \beta_{1k} E_{1jk} = 0 \quad j = 1, 2, \cdots n_b \quad (37)$$

$$\sum_{k=1}^{n_T} \beta_{1k} E_{2jk} = 0 \quad j = 1, 2, \cdots n_b \tag{38}$$

$$\sum_{k=1}^{n_T} \beta_{1k} E_{3jk} = 0 \quad j = 1, 2, \cdots n_b \tag{39}$$

where (if the higher order terms are neglected)

$$\begin{aligned}
A_{1ik} &= \frac{1}{R_e}\nabla^2\Psi_k(\mathbf{x}_i) - U_0(\mathbf{x}_i)\frac{\partial\Psi_k}{\partial X}(\mathbf{x}_i) - V_0(\mathbf{x}_i)\frac{\partial\Psi_k}{\partial Y}(\mathbf{x}_i) - \frac{\partial U_0}{\partial X}\Psi_k(\mathbf{x}_i) \\
A_{2ik} &= -\frac{\partial U_0}{\partial Y}(\mathbf{x}_i)\Psi_k(\mathbf{x}_i) \\
A_{3ik} &= -\frac{\partial\Psi_k}{\partial X}(\mathbf{x}_i) \\
B_{1ik} &= -\frac{\partial V_0}{\partial X}(\mathbf{x}_i)\Psi_k(\mathbf{x}_i) \\
B_{2ik} &= \frac{1}{R_e}\nabla^2\Psi_k(\mathbf{x}_i) - U_0(\mathbf{x}_i)\frac{\partial\Psi_k}{\partial X}(\mathbf{x}_i) - V_0(\mathbf{x}_i)\frac{\partial\Psi_k}{\partial Y}(\mathbf{x}_i) - \frac{\partial V_0}{\partial Y}\Psi_k(\mathbf{x}_i) \\
B_{3ik} &= -\frac{\partial\Psi_k}{\partial Y}(\mathbf{x}_i) \\
C_{1ik} &= -\frac{\partial V_0}{\partial Y}(\mathbf{x}_i)\frac{\partial\Psi_k}{\partial X}(\mathbf{x}_i) + \frac{\partial V_0}{\partial X}(\mathbf{x}_i)\frac{\partial\Psi_k}{\partial Y}(\mathbf{x}_i) \\
C_{2ik} &= -\frac{\partial U_0}{\partial X}(\mathbf{x}_i)\frac{\partial\Psi_k}{\partial Y}(\mathbf{x}_i) + \frac{\partial U_0}{\partial Y}(\mathbf{x}_i)\frac{\partial\Psi_k}{\partial X}(\mathbf{x}_i) \\
C_{3ik} &= \frac{1}{2}\nabla^2\Psi_k(\mathbf{x}_i) \\
F_{1i} &= U_0(\mathbf{x}_i)\frac{\partial U_0}{\partial X}(\mathbf{x}_i) + V_0(\mathbf{x}_i)\frac{\partial U_0}{\partial Y}(\mathbf{x}_i) + \frac{\partial P_0}{\partial X}(\mathbf{x}_i) \\
F_{2i} &= U_0(\mathbf{x}_i)\frac{\partial V_0}{\partial X}(\mathbf{x}_i) + V_0(\mathbf{x}_i)\frac{\partial V_0}{\partial Y}(\mathbf{x}_i) + \frac{\partial P_0}{\partial Y}(\mathbf{x}_i) \\
F_{3i} &= 0 \\
E_{ljk} &= \Psi_k(\mathbf{x}_j) \quad \text{if} \quad \mathbf{x}_j \in \Gamma_{\Phi_l} \\
E_{ljk} &= \frac{\partial\Psi_k}{\partial n}(\mathbf{x}_j) \quad \text{if} \quad \mathbf{x}_j \in \Gamma_{Q_l}
\end{aligned}$$

In the above $\Phi \equiv (U, V, P)$; $Q \equiv (\partial U/\partial n, \partial V/\partial n, \partial P/\partial n)$; $n_T = 3(n_b + n_d)$, and $\mathbf{x}_i \equiv (X, Y)$ for 2D flows.

TEST RESULTS

We examined the lid-driven cavity flow problem depicted in Fig. 1. A unit horizontal velocity is imposed on the lid (at $Y^* = 1$), while the no-slip boundary condition $U^* = V^* = 0$ is imposed on all solid walls. The boundary condition for the pressure on all walls is (*Fletcher* [1991]):

$$\frac{\partial P}{\partial n} = \frac{1}{R_e}\frac{\partial}{\partial s}\left(\frac{\partial U^*}{\partial Y^*} - \frac{\partial V^*}{\partial X^*}\right)$$

A typical convergence profile, using Approach I, is shown ($R_e = 15$) in Fig. 2. The horizontal velocity at the vertical center-line is shown in Fig. 3.

CONCLUSIONS

A boundary element code, based on the use of global interpolation functions, for solving the Navier Stokes equations have been proposed in this paper. The avoidance of any domain integration shows the enormous power of the technique. As long as the underlying physics of the problem is adequately represented in the fundamental solutions used as the kernel of the integral equations, accurate simulations can be carried out for moderate to high Reynold's number flows. Only trigonometric bases have been used to represent the nonlinear convective terms. Investigations are currently underway for employing other bases including those derived from orthogonal functions such Chebychev polynomials, wavelets, and cellular automata transforms. Three-dimensional GIF-based BEM code for internal flows are also being developed.

Acknowledgments

This investigation has been supported by NASA (Lewis Research Center) under the Contract NAS3-27019.

REFERENCES

1. Brebbia, C.A., *Two Different Approaches for Transforming Domain Integrals to the Boundary*. Mathl Comput. Modelling, Vol. 15, No. 3-5, pp. 43-58, 1991.

2. Brebbia, C.A., J.C.F. Telles, and L.C. Wrobel, **Boundary Element techniques - Theory and applications in Engineering**. Springer-Verlag, 1984.

3. Cheng, A. H-D., S. Grilli, and O. Lafe. *Dual Reciprocity Boundary Element Based on Global Interpolation Functions*. Eng. Analysis with Boundary Elements, to appear, 1994.

4. Cheng, A. H-D., and D. Ouazar. *Groundwater*. Chapter 9 in **Boundary Element Techniques in Geomechanics**, eds. G.D. Manolis and T.G. Davies, CMP/Elsevier, 1993.

5. Fletcher. C.A.J., **Computational Techniques for Fluid Dynamics**, Vol. II (pg. 391), Springer-Verlag. 1991.

6. Greenberg. M.D., **Applications of Green's Functions in Science and Engineering**, Prentice-Hall. Englewood Cliffs, New Jersey, 1971.

7. Jaswon, M.A., and G.T. Symm. *Integral Equation Methods in Potential Theory and Elastostatics*. Academic. San Diego, Calif., 1977.

8. Lafe, O., *A Dual Reciprocal Boundary element Formulation for Viscous Flows*, in Proc. NASA Fifth Annual Thermal and Fluids Analysis Workshop (NASA Conference Publication 10122), Brook Park, Aug. 16-20, 1993.

9. Lafe, O., and A. H-D. Cheng, *A Global Interpolation Function Based Boundary Element Method for Deterministic, Non-homogeneous, and Stochastic Flows in Porous Media*. Computers and Structures, To Appear, 1994.

10. Nardini, D., and C.A. Brebbia. *A New Approach to Free Vibration Analysis using Boundary Elements*, in **Boundary Element Methods in Engineering**, Proc. 4th Int. Sem., Southampton, ed. C.A. Brebbia, Springer-Verlag, 312-326, 1982.

11. Partridge, P.W., C.A. Brebbia, and L.C. Wrobel. *The Dual Reciprocity Boundary Element Method*. CMP/Elsevier, 1992.

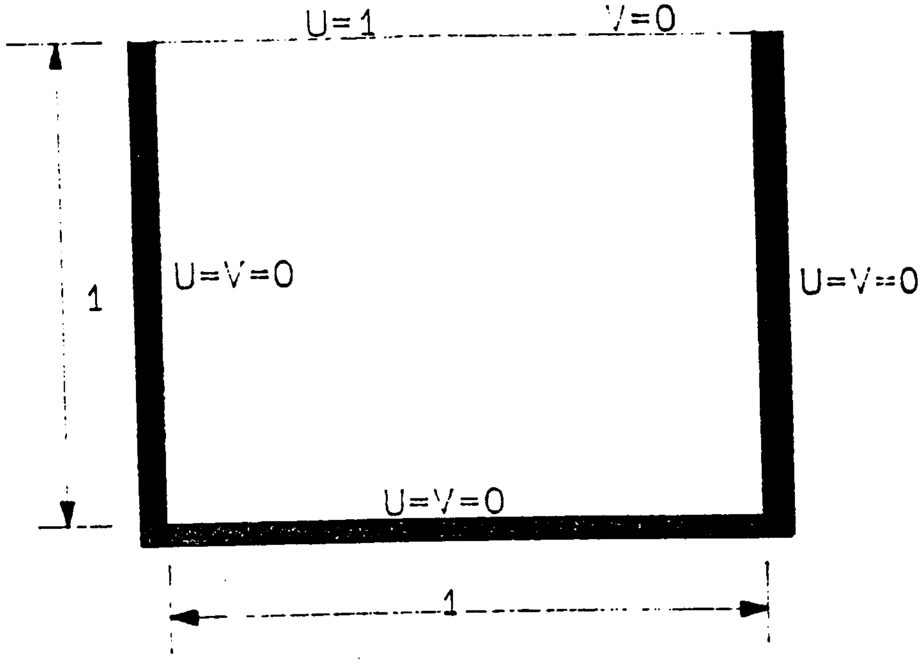

Figure 1: Lid-driven Cavity Problem

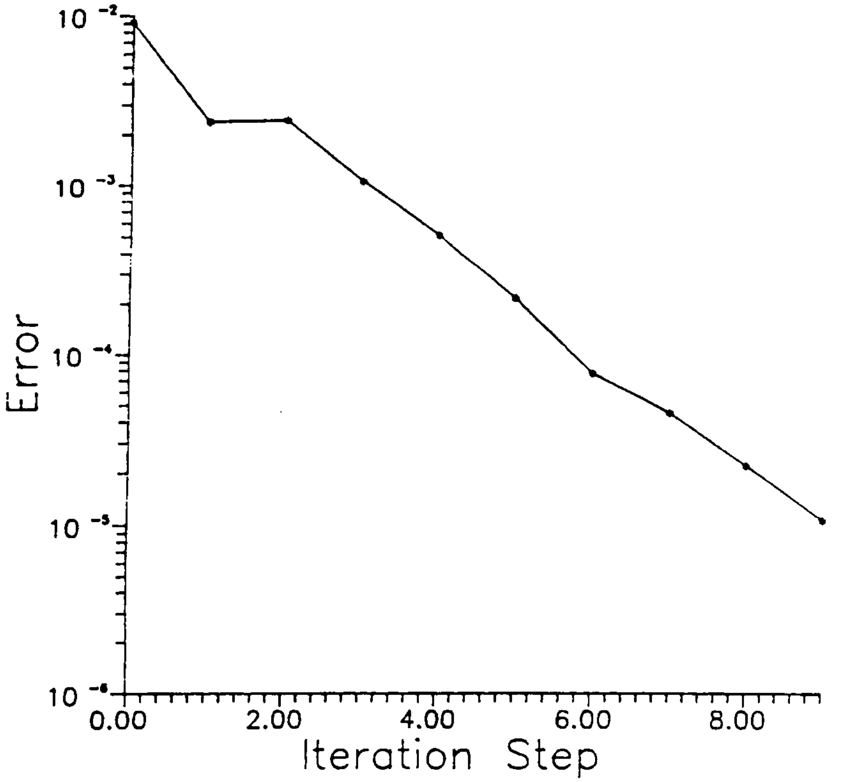

Figure 2: Typical Convergence Profile

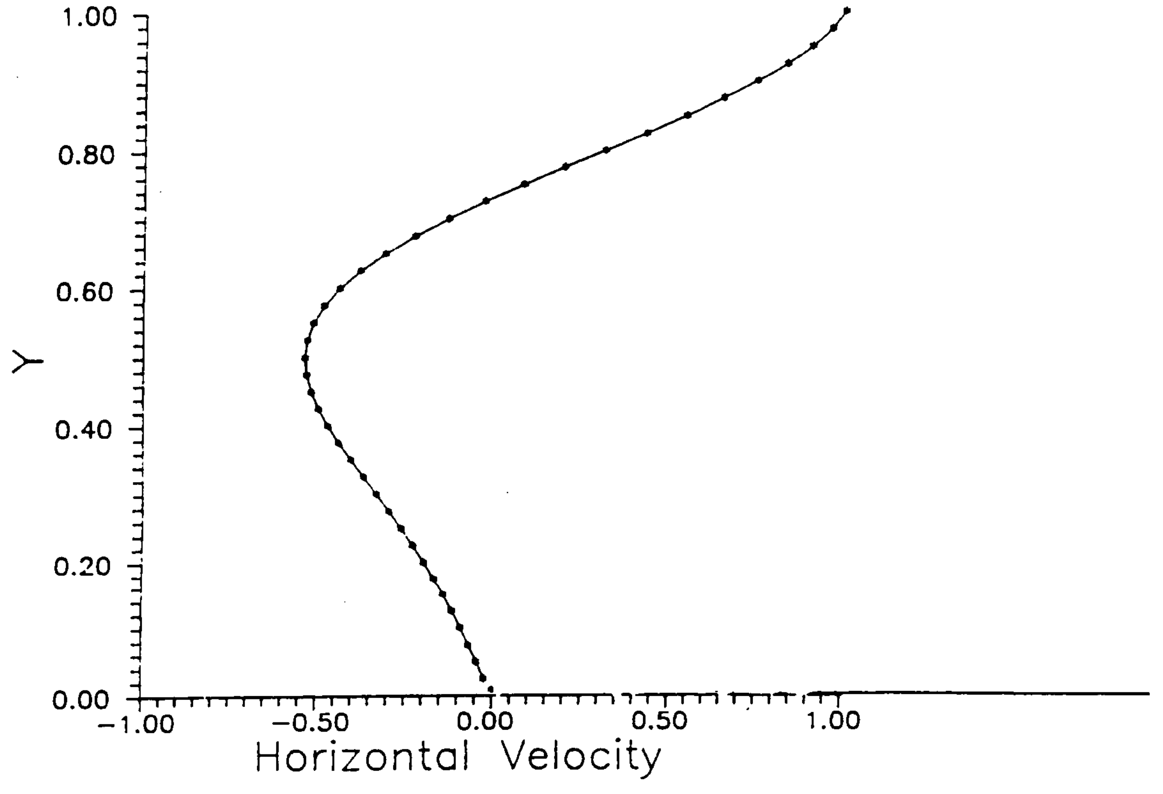

Figure 3: Horizontal Velocity at Vertical Center-Line